© 2022. Published by The Company of Biologists Ltd | Journal of Experimental Biology (2022) 225, jeb244659. doi:10.1242/jeb.244659

RESEARCH ARTICLE

Metabolic rate increases with acclimation temperature and is associated with mitochondrial function in some tissues of threespine stickleback

Louise Cominassi*,‡, Kirsten N. Ressel*, Allison A. Brooking, Patrick Marbacher, Eleanor C. Ransdell-Green and Kristin M. O'Brien

ABSTRACT

The metabolic rate ($\dot{M}_{O_2}$) of eurythermal fishes changes in response to temperature, yet it is unclear how changes in mitochondrial function contribute to changes in $\dot{M}_{O_2}$. We hypothesized that $\dot{M}_{O_2}$ would increase with acclimation temperature in the threespine stickleback (*Gasterosteus aculeatus*) in parallel with metabolic remodeling at the cellular level but that changes in metabolism in some tissues, such as liver, would contribute more to changes in $\dot{M}_{O_2}$ than others. Threespine stickleback were acclimated to 5, 12 and 20°C for 7 to 21 weeks. At each temperature, standard and maximum metabolic rate (SMR and MMR, respectively), and absolute aerobic scope (AAS) were quantified, along with mitochondrial respiration rates in liver, oxidative skeletal and cardiac muscles, and the maximal activity of citrate synthase (CS) and lactate dehydrogenase (LDH) in liver, and oxidative and glycolytic skeletal muscles. SMR, MMR and AAS increased with acclimation temperature, along with rates of mitochondrial phosphorylating respiration in all tissues. Low SMR and MMR at 5°C were associated with low or undetectable rates of mitochondrial complex II activity and a greater reliance on complex I activity in liver, oxidative skeletal muscle and heart. SMR was positively correlated with cytochrome *c* oxidase (CCO) activity in liver and oxidative muscle, but not mitochondrial proton leak, whereas MMR was positively correlated with CCO activity in liver. Overall, the results suggest that changes in $\dot{M}_{O_2}$ in response to temperature are driven by changes in some aspects of mitochondrial function in some, but not all, tissues of threespine stickleback.

KEY WORDS: Eurythermal, *Gasterosteus aculeatus*, Aerobic scope, Mitochondria, Thermal plasticity

INTRODUCTION

Temperature is a key environmental driver of metabolic rate ($\dot{M}_{O_2}$) in ectothermic organisms (Clarke and Johnston, 1999). Despite having a body temperature defined by the environmental temperature, many cold-temperate fish species occupy habitats where temperature fluctuations, sometimes as great as 20°C, occur daily and seasonally. Although acute changes in temperature immediately alter $\dot{M}_{O_2}$ of fishes owing to the thermodynamic effect of temperature on the catalytic rate of enzymes, many fishes are capable of physiological acclimation, modifying enzyme activities, tissue and organ mass, and membrane composition to maintain $\dot{M}_{O_2}$ and rates of ATP synthesis across a broad range of temperatures (Guderley, 1990).

The extent of thermally induced metabolic remodeling varies among tissue types and organs in fishes (Chung et al., 2017; O'Brien, 2011). For example, in the threespine stickleback, *Gasterosteus aculeatus*, metabolic remodeling differs between oxidative skeletal muscle and liver (Orczewska et al., 2010). In response to cold acclimation to 8°C, mitochondrial density increases 1.9-fold in oxidative skeletal muscle but is unchanged in liver (Orczewska et al., 2010). Nevertheless, when measured at a common temperature, the maximal activities of cytochrome *c* oxidase (CCO) and citrate synthase (CS), two aerobic metabolic enzymes localized to mitochondria, are higher in both liver and oxidative skeletal muscle in cold-acclimated compared with warm-acclimated stickleback (Orczewska et al., 2010). However, there are subtle differences in the magnitude of change in enzyme activities, with CCO activity increasing to a greater extent in oxidative muscle than in liver, and CS activity increasing more so in liver than in oxidative muscle (Orczewska et al., 2010). Similarly, there are tissue-specific changes in mitochondrial function in response to temperature in the southern catfish (*Silurus meridionalis*), where mitochondrial state III (phosphorylating) respiration rates and CCO activity are higher in the heart, kidney and liver, but not in the brain and glycolytic muscle of animals acclimatized to winter conditions (12.5°C) compared with those held in summer conditions (27.5°C) when measured at a common temperature (Yan and Xie, 2015).

Metabolic remodeling at the cellular level in response to changes in temperature leads to changes in $\dot{M}_{O_2}$. Basal metabolic rate, which reflects the cost of maintaining homeostasis, is commonly defined as standard metabolic rate (SMR) and is measured as the minimal oxygen consumption in resting, post-absorptive fish (Chabot et al., 2016a). Aerobic capacity, or absolute aerobic scope (AAS), represents the ability of the animals to deliver oxygen to tissues above their basic requirement and is calculated as the difference between maximum metabolic rate (MMR) and SMR (Farrell et al., 2009; Norin and Clark, 2016). In response to an acute increase in temperature, both SMR and MMR increase, but MMR reaches a maximum at lower temperatures compared with SMR, resulting in a loss of AAS above (and below) a thermal optimum (T_{opt}) (Farrell et al., 2009; Steinhausen et al., 2008). Similar to cellular metabolism, AAS is malleable with acclimation, resulting in adjustments in AAS, T_{opt} (Hvas et al., 2017; Sandblom et al., 2014; Scheuffele et al., 2021) and the thermal breadth of AAS in some cases (Ferreira et al., 2014), although not always (Healy and Schulte, 2012). Because AAS represents an organism's capacity for exercise, for those species that depend on a high AAS to support

University of Alaska Fairbanks, Institute of Arctic Biology, PO Box 757000 Fairbanks, AK 99775, USA.
*These authors contributed equally to this work

‡Author for correspondence (lmcominassi@alaska.edu)

L.C., 0000-0002-2606-4753; K.M.O., 0000-0002-3311-0690

Received 14 June 2022; Accepted 7 October 2022

Journal of Experimental Biology (2022) 225, jeb244659. doi:10.1242/jeb.244659

intense bouts of exercise, such as during migration or foraging, AAS may influence fitness (Brownscombe et al., 2017).

Studies integrating measurements of both $\dot{M}_{O_2}$ and cellular metabolism have revealed that some tissues and metabolic processes contribute more to SMR and MMR than others. For example, in brown trout (*Salmo trutta*), intraspecific variation in MMR is positively correlated with mitochondrial leak respiration and CCO activity in glycolytic skeletal muscle (Salin et al., 2016) and CCO activity in liver (Norin and Malte, 2012), whereas variation in SMR is associated with mitochondrial leak rate in liver (Salin et al., 2016) and CCO and CS activity in liver (Norin and Malte, 2012). Additionally, MMR and T_{opt} of AAS are associated with cardiac performance (Farrell et al., 2009; Steinhausen et al., 2008) and cardiac aerobic metabolic capacity in several fish species (O'Brien et al., 2018; Pichaud et al., 2017, 2019; Ressel et al., 2022).

Although metabolic remodeling at the cellular level in response to thermal acclimation has been well described for many fish species (Egginton and Sidell, 1989; Fangue et al., 2008; Pichaud et al., 2017), it is not always clear how adjustments at the cellular level contribute to whole-organism changes in $\dot{M}_{O_2}$. For example, in the common intertidal triplefin fish (*Forsterygion lapillum*), there is no association between mitochondrial function and SMR or MMR in response to thermal acclimation (Khan et al., 2014). In catfish, despite increases in mitochondrial function in kidney, liver and cardiac muscle in response to warm acclimation (Yan and Xie, 2015), resting metabolic rate remains unchanged by acclimation (Yan and Xie, 2011), although brain and glycolytic skeletal muscle mitochondrial state 3 respiration rates are also unchanged by acclimation, suggesting that mitochondrial function in some tissues and organs may contribute more than others to $\dot{M}_{O_2}$ (Yan and Xie, 2015).

Identifying the molecular and cellular basis of thermally induced changes in SMR and MMR would provide a foundation for identifying the molecular drivers of metabolic remodeling and contribute towards understanding the limits of thermal tolerance. The aim of the present study was to characterize changes in metabolism in response to temperature and determine how reorganization at the cellular level contributes to adjustments in $\dot{M}_{O_2}$ in threespine stickleback. Based on previous studies (Orczewska et al., 2010; Ressel et al., 2022), we hypothesized that AAS would increase with an increase in acclimation temperature and be associated with metabolic remodeling at the cellular level, with some tissues undergoing greater remodeling and contributing more to changes in $\dot{M}_{O_2}$ than others. The threespine stickleback is an ideal model organism for these studies because it inhabits thermally variable environments ranging from the North Slope of Alaska to the Baja Peninsula of Mexico (Wootton, 1984). Stickleback inhabiting lakes in central Alaska, where animals for these studies were collected, experience seasonal temperatures ranging between 4 and ∼25°C (Fig. S1). Stickleback were acclimated to 5, 12 and 20°C for 7–21 weeks. SMR, MMR and AAS were quantified at each acclimation temperature along with mitochondrial function in permeabilized liver and oxidative skeletal muscle in the same animals. In a different set of animals, mitochondrial function was measured in the heart, and in a third set of animals, the maximal activities of the key metabolic enzymes citrate synthase (CS) and lactate dehydrogenase (LDH) were quantified in liver and oxidative and glycolytic skeletal muscles.

List of symbols and abbreviations

AAS	absolute aerobic scope
Abs	absolute
BL	body length
CCO	rate of uncoupled oxidative phosphorylation through cytochrome *c* oxidase (complex IV)
CS	citrate synthase
CV_{MLND}	coefficient of variation of the mean of the lowest normal distribution
D	density of animal
Dim	dimension
DO	dissolved oxygen
ETS	electron transport system; rate of uncoupled respiration through all complexes
FAS	factorial aerobic scope
K	Fulton's condition factor
L	liver
LDH	lactate dehydrogenase
LEAKOmy	rate of leak respiration in the presence of oligomycin
L_s	standard length
M_b	wet body mass
MLND	mean of the lowest normal distribution
MMR	maximum metabolic rate
$\dot{M}_{O_2}$	metabolic rate
OxM	oxidative skeletal muscle
OXP I	rate of phosphorylating respiration supported by complex I
OXP I,II	rate of phosphorylating respiration supported by complexes I and II
OXP II	rate of phosphorylating respiration through complex II
PCA	principal component analysis
Q_{10}	temperature coefficient
SMR	standard metabolic rate
SUIT	substrate-uncoupler-inhibitor titration
T_{opt}	temperature optimum
Trunc	truncated
V	total volume of the respirometer
V_{max}	maximum velocity

MATERIALS AND METHODS

Stickleback capture and acclimation

Threespine stickleback (*Gasterosteus aculeatus* Linnaeus 1758) were collected in September 2020 from Nancy Lake, Alaska, USA (61.692°N, 150.020°W), using minnow traps. Animals were transported to the University of Alaska Fairbanks (UAF), where they were maintained in recirculating 30-gallon (=113.56 l) tanks (17–21 animals per tank) filled with deionized water supplemented with 0.35 ppt Instant Ocean. Animals were held at 17°C for 1 mo, until the water chemistry in the tanks stabilized, then acclimated to 5, 12 or 20°C by changing the temperature in the tanks at a rate of 3°C per day by adjusting the temperature in the environmental chamber (5 and 12°C) or room (20°C). Three tanks were maintained at each temperature and animals were randomly selected from tanks for experiments. All animals were held on a 10 h:14 h light:dark cycle and fed twice daily a diet of blood worms. All procedures were approved by the UAF Institutional Animal Care and Use Committee (1253621-22).

Organismal respirometry

$\dot{M}_{O_2}$ was measured in 19 individuals (n=6, 6 and 7 for the 5, 12 and 20°C acclimation groups, respectively) between weeks 7 and 17 of acclimation. Measurements were conducted using a 170 ml glass Loligo swim tunnel respirometer (Loligo Systems, Viborg, Denmark) with toxic-free polyvinyl chloride tubing (chamber volume=184 ml, tube volume=1.24 ml). The ratio of body mass to total respirometer volume (chamber volume+tube volume) ranged from 1:93 to 1:265. Organismal respirometry trials were conducted on one animal at a time in the environmental chamber or room in which the animals were held, alternating among temperature groups.

The respirometer was shrouded in black plastic to minimize disturbance. Water temperature in the respirometer was measured once per second and was maintained at the acclimation temperature by circulating water through a stainless-steel chilling coil submerged in a cooler filled with ice water. A dipping probe mini oxygen sensor was connected to a Witrox 1 oxygen meter (Loligo Systems) to measure dissolved oxygen (DO) levels once per second. The oxygen sensor was placed within the inner chamber of the respirometer and calibrated for each experiment at the acclimation temperature to 100% air saturation using vigorously aerated water in the respirometer and 0% air saturation using 2% sodium sulfite. The respirometer was drained and rinsed with deionized water at the conclusion of each experiment and sanitized with a dilute bleach solution every fourth trial to minimize background microbial respiration rates. The water current velocity in the swim tunnel respirometer was calibrated by recording and measuring the flow rate of green fluorescent microbeads between 100 and 400 rpm at 100 rpm intervals following the manufacturer's protocol.

Animals were fasted for 36 h, measured for standard length (cm) and body mass (g), and then placed into the respirometer and allowed to recover from the stress of handling for 1 h. Fish were induced to swim by increasing the water velocity from 0 to 45 cm s^{-1} (0 to 9.04 BL s^{-1}; the velocity limit of the respirometer) to confirm that each fish was capable of swimming at 45 cm s^{-1}. The velocity was then reduced to ∼100 rpm [mean±s.d.=0.81±0.14 cm s^{-1} (0.16±0.03 BL s^{-1})] to circulate water in the chamber but still allow the fish to maintain its position without swimming. Animals were allowed to recover for at least 6 h prior to measuring DO overnight for 10 h to quantify SMR using intermittent flow respirometry with the following settings: flush for 7 min, wait for 1 min and measure for 28, 15 or 12 min at 5, 12 and 20°C, respectively.

The following day, MMR was measured by increasing the velocity by 10% of the fish's maximum velocity (V_{max}) every 2 min until 40% V_{max} was attained. Thereafter, $\dot{M}_{O_2}$ was measured using intermittent respirometry with the following settings: 2 min flush, 1 min wait and 5 min measure. If the fish was not swimming at the onset of the wait period, it was induced to swim by decreasing the velocity to 0 cm s^{-1} and then immediately increasing it to the target velocity for that cycle as described in Ressel et al. (2022). Oxygen consumption was measured at each velocity for two cycles before increasing the velocity by 10% V_{max} until the fish could no longer right itself or was repeatedly unable or unwilling to burst swim. If the fish completed two cycles at V_{max} and was still not fatigued, the fish was induced to swim every time it stopped swimming until it was fatigued for one additional cycle. If the fish became fatigued during a measurement period, the velocity was decreased to 100 rpm for the remainder of the period plus one additional cycle following fatigue. MMR trials lasted for 110±24 min (mean±s.d.) for each animal. DO was maintained above 84% saturation for all trials and always returned to 100% saturation during the flush period.

Background microbial respiration rates were measured twice before and twice after each trial with the following settings: 5 min flush, 1 min wait and 30 min measure. Replicates were averaged and background respiration rates interpolated using a linear correction (package: FishResp; function: correct.meas; method: 'linear'). Regions of the data (or an entire measurement period if necessary) for which DO levels increased were removed prior to calculating background respiration rates. For some trials, DO levels always increased and for these trials, background rates of respiration were set to zero. Mean±s.d. background respiration was 2.5±2.5% of the SMR estimate for that measurement period (max.=15.0%).

Calculating SMR and MMR

Organismal respirometry data were collected using AutoResp version 2.3.0 (Loligo Systems) and processed using RStudio version 1.3.1093 (www.rstudio.com/) operating with R version 4.0.3. Code was modified from the FishResp package version 1.0.3 (Morozov et al., 2019) to import respirometry data into R and correct raw data for background $\dot{M}_{O_2}$.

The slope of a linear model fit to the background corrected DO values for each measurement period (package: FishResp; function: extract.slope; method: 'all') was used to estimate metabolic rate (package: FishResp; function: calculate.MR). All SMR and MMR estimates accounted for the body mass, density and volume of the organism, as well as the total volume of the respirometer based on the following equation:

$$\dot{M}_{O_2,mass} = ((\Delta[O_2]/\Delta t) \times (V - D \times M_b)) \times M_b^{-1}, \quad (1)$$

where $\Delta[O_2]/\Delta t$ is the slope (mg O_2 l^{-1} h^{-1}), V is the total volume of the respirometer (l), D is the density of the animal (default of 1 kg l^{-1} used for all animals) and M_b is wet body mass (kg) (eqns 1 and 2 in Morozov et al., 2019).

Between 16 and 30 estimates of SMR were obtained for each animal. The SMR values were obtained according to methods described in Ressel et al. (2022). Briefly, DO values were smoothed as suggested by Chabot et al. (2021) and cycles with r^2<0.95 were removed. The final SMR estimate for each animal was calculated using the mean of the lowest normal distribution (MLND) when the coefficient of variation of MLND (CV_{MLND})≥5.4, and the 20% quantile method when CV_{MLND}≤5.4 (Chabot et al., 2016b; Reemeyer and Rees, 2019).

We attempted to use an iterative algorithm to calculate MMR (Zhang et al., 2019); however, the CV and s.d. were high and equivalent for the 17 sampling windows examined between 0.5 and 5 min. Therefore, we calculated MMR by fitting DO to a linear model to estimate the slope of the line (Norin and Clark, 2016; Rosewarne et al., 2016; Rummer et al., 2016). The entire (5 min) measurement period that yielded the highest estimate was chosen as MMR (hereafter referred to as 'traditional MMR'; Norin and Clark, 2016; Rosewarne et al., 2016; Rummer et al., 2016). We also employed a second approach (hereafter referred to as 'truncated MMR'), in which each measurement period was edited to retain only the steepest declines in DO as long as there was a minimum of 100 s (33% of the measurement period) of data remaining (mean±s.d.=225±78 s, range=100–300 s) and processed as described above (Ressel et al., 2022; Rummer et al., 2016).

Absolute aerobic scope (AAS) was calculated as MMR−SMR.

Mitochondrial respirometry

Mitochondrial respiration rates in liver tissues and oxidative muscle fibers were performed on the same fish as those used for organismal respirometry ($\dot{M}_{O_2}$), with additional animals sampled between weeks 17 and 20 [2 (for muscle), 4 (2 for muscle, 2 for liver) and 1 (for muscle) from the 5, 12 and 20°C temperature groups, respectively] to increase the sample size because of the larger variation in mitochondrial measurements compared with measurements of $\dot{M}_{O_2}$, especially in muscle. Mitochondrial respiration rates in heart ventricle were only measured in animals acclimated to 5 (n=12) and 12°C (n=13) because there were an insufficient number of animals acclimated to 20°C. These animals

were harvested between weeks 18 and 20 and were not used for measuring $\dot{M}_{O_2}$. Hearts from two individuals were pooled to obtain sufficient material except for one 12°C acclimated animal, whose heart was sufficiently large.

Animals were euthanized for mitochondrial respirometry with an intentional overdose of 0.05% tricaine methanesulfonate adjusted to pH 7 with bicarbonate. Liver tissues, oxidative muscle fibers and heart ventricles were permeabilized with saponin as described by Iftikar et al. (2014), modified slightly to maintain the integrity of the inner mitochondrial membrane. Liver tissues were diced and muscle fibers and ventricles were teased apart in 4 ml chilled BIOPs buffer (2.77 mmol l^{-1} CaK_2 EGTA, 7.23 mmol l^{-1} K_2 EGTA, 5.77 mmol l^{-1} Na_2 ATP, 6.56 mmol l^{-1} $MgCl_2 \cdot 6H_2O$, 20 mmol l^{-1} taurine, 20 mmol l^{-1} imidazole, 0.5 mmol l^{-1} DTT and 50 mmol l^{-1} KMES, with 15 mmol l^{-1} NaPCr added to the buffer for muscle fibers and ventricles) on ice. Saponin was added as follows: liver tissues from animals acclimated to 5 and 12°C were treated with 25 µg ml^{-1} saponin in BIOPS for 12 min, muscle fibers with 50 µg ml^{-1} saponin in BIOPS for 20 min and ventricles with 37.5 µg ml^{-1} saponin in BIOPS for 15 min on ice with gentle shaking. Liver tissues from 20°C animals were treated with saponin in BIOPS buffer for 15 min and muscle fibers for 25 min. Permeabilized tissues were washed three times (once briefly, and twice for 10 min each) with mitochondrial respiration medium adjusted to pH 7.2 (MiRO5: 0.5 mmol l^{-1} EGTA, 3 mmol l^{-1} $MgCl_2$, 60 mmol l^{-1} lactobionic acid, 20 mmol l^{-1} taurine, 10 mmol l^{-1} KH_2PO_4, 20 mmol l^{-1} HEPES, 110 mmol l^{-1} D-sucrose and 1 g l^{-1} BSA) and then blotted on weighing paper to remove excess moisture, weighed and added to the respirometry chambers.

Mitochondrial function was measured at the acclimation temperature of the animal (5, 12 or 20°C) using an Oroboros O2k high resolution respirometer (Oroboros Instruments, Innsbruck, Austria) following a substrate-uncoupler-inhibitor titration (SUIT) protocol (Doerrier et al., 2018). Electrodes were calibrated with sodium dithionite each day to 0% and each week to 100% air saturation. Background oxygen flux was determined at each temperature as needed. Oxygen was added to the gas phase above the medium (MiRO5) so that O_2 levels were maintained between 250 and 450 nmol ml^{-1}. Pyruvate (10 mmol l^{-1}) and malate (2 mmol l^{-1}) were added as substrates for complex I, and O_2 consumption was measured to assess the oxygen flux of the initial resting state in the absence of ADP. This was followed by additions of ADP (10 mmol l^{-1} for liver tissues, 12.5 mmol l^{-1} for muscle and ventricles) and then aliquots of 2.5 mmol l^{-1} ADP until saturating levels were achieved to measure maximum state III respiration rates (OXP I). Cytochrome *c* (10 µmol l^{-1}) was then added to assess the integrity of the outer membrane; the rate of oxygen flux never increased by more than 15% after the addition of cytochrome *c*. Succinate (10 mmol l^{-1}) was then added to measure rates of respiration supported by complexes I and II (OXP I,II). ATP synthase was then inhibited to measure state IV respiration and the rate of leak (LEAKOmy) by adding 1 µg ml^{-1} oligomycin to liver tissues and ventricles and 2 µg ml^{-1} to muscle. Maximal flux through the electron transport system (ETS) was measured by the addition of repeated titrations of the uncoupler carbonyl cyanide *p*-(trifluoromethoxy) phenyl-hydrazone (FCCP) (4 µmol l^{-1} for muscle, 3 µmol l^{-1} for liver tissue and ventricle) until maximum rates were achieved. Complex I was inhibited by the addition of rotenone (1 µmol l^{-1} for muscle, 0.5 µmol l^{-1} for liver and ventricle) and complex III by the addition of antimycin A (5 µmol l^{-1}). Ascorbate (2 mmol l^{-1}) and *N*,*N*,*N*′,*N*′-tetramethyl-*p*-phenylenediamine (TMPD) (0.5 mmol l^{-1}) were then added to measure the activity of complex IV (CCO). Background rates of autooxidation of TMPD were determined by addition of sodium azide (200 mmol l^{-1}).

Mitochondrial respiration rates were normalized to the wet mass (mg) of the tissue and corrected for background oxygen flux measured at each experimental temperature. Respiration rates that were negative after the background correction were assumed to be zero.

Enzymology

Animals used for enzyme assays were euthanized after 21 weeks of acclimation by immersion in liquid nitrogen and then stored at −80°C. Tissues were homogenized on ice using Ten Broeck hand-held homogenizers (Corning, Glendale, AZ, USA) in 40 mmol l^{-1} HEPES, 1 mmol l^{-1} EDTA and 2 mmol l^{-1} $MgCl_2$ (and 2 mmol l^{-1} DTT for LDH assays) at pH 7.8 and frozen at −80°C until further analysis. Maximal enzymatic activities were measured at the acclimation temperature using a Lamda 40 spectrophotometer (Perkin-Elmer, Waltham, MA, USA) equipped with a refrigerated, circulating water bath except for CS activity at 20°C, which was measured using a SpectraMax Plus 384 microplate reader (Molecular Devices, San Jose, CA, USA). Changes in absorbance were monitored for 3 min in the absence of substrate (background activity) and for 3 min following the addition of substrate. Measurements were made in triplicate (n=6 per temperature group) and activity was expressed as µmol l^{-1} product min^{-1} g^{-1} wet mass.

Citrate synthase

Maximal activity of CS (EC 2.3.3.1) was measured following a modified method by Srere et al. (1963). The final assay reaction mixture contained 75 mmol l^{-1} Tris, 0.25 mmol l^{-1} 5,5 -dithiobis-2-nitrobenzoic acid (DTNB), 0.40 mmol l^{-1} acetyl coenzyme A and 0.5 mmol l^{-1} oxaloacetate, adjusted to pH 8.0. The oxidation of DTNB was initiated by the addition of oxaloacetate and monitored at 412 nm.

Lactate dehydrogenase

Maximal activity of LDH (EC 1.1.1.27) was measured following a modified method by Hansen and Sidell (1983). The final assay reaction mixture contained 50 mmol l^{-1} imidazole, 1 mmol l^{-1} potassium cyanide (KCN), 0.15 mmol l^{-1} NADH and 2.5 mmol l^{-1} sodium pyruvate, adjusted to pH 7.7. The oxidation of NADH was initiated by the addition of sodium pyruvate and monitored at 340 nm.

All biochemicals were purchased from Sigma-Aldrich (St Louis, MO, USA).

Calculations

Fulton's condition factor was calculated as:

$$K = M_b/L_s^3 \times 100, \quad (2)$$

where M_b is the wet body mass of the fish (g) and L_s is the standard length (cm).

The temperature coefficient (Q_{10}) was calculated as:

$$Q_{10} = (R_2/R_1)^{10/(T_2-T_1)}, \quad (3)$$

where R_1 and R_2 are the mean measurements from all animals at temperature T_1 or T_2, respectively.

Statistical analyses

Unless otherwise noted below, statistical analyses were conducted and graphs were produced using Prism v.9 (Graphpad Software Inc., San Diego, CA, USA). Significance was accepted when $P<0.05$. Data were analyzed for outliers using Grubbs test, for normality with the Shapiro–Wilk test, and for equal variance with a Bartlett test or *F*-test. Data were transformed to meet normality requirements when possible. To compare measurements among the three temperature acclimation groups, a one-way ANOVA followed by Tukey's honest significant difference test was conducted when data were normally distributed and had equal variance. A Kruskal–Wallis test followed by Dunn's multiple comparisons test was used to compare acclimation groups when they were not. A Brown–Forsythe ANOVA followed by a Dunnett's T3 multiple comparisons test was used when the data were normally distributed but variance was unequal. For measurements, such as those in the heart, that were conducted for only two temperature groups (5 and 12°C), significant differences were identified with a Student's *t*-test or a *t*-test with Welch's correction when there was unequal variance between the two groups.

Physical characteristics

Physical characteristics (body mass, length and condition factor) were compared among temperature acclimation groups for each experiment (metabolic rate/liver and oxidative muscle mitochondrial function, heart mitochondrial function and enzyme assays) because animals were harvested at different times for each experiment.

SMR, MMR and AAS

Because organismal respirometry trials were completed over a span of 10 weeks, a simple linear regression was used to determine whether SMR or MMR varied over the duration of the experiments. A paired *t*-test was used to determine whether MMR estimates differed when calculated using the traditional or truncated method.

Integration of metabolic rate and mitochondrial function

A principal component analysis (PCA) was used to characterize the relationship between SMR or MMR and mitochondrial function in liver and oxidative skeletal muscle (OXP I,II, LEAKOmy and CCO) using the FactoMineR R package processed with the RStudio version ETS, n 1.3.1093.

Correlations between SMR or MMR and mitochondrial function in the liver and oxidative skeletal muscle (logOXP I,II, LEAKOmy and CCO) were evaluated using Pearson's *r* test. Absolute SMR (abs SMR) and absolute MMR (abs MMR) from FishResp were used and mass was added to the model as a predictor variable. The logOXP I,II and LEAKOmy were first normalized to mitochondrial content by dividing by the CCO rate to avoid potential collinearity between mitochondrial properties (logOXP I,II/CCO and LEAKOmy/CCO, respectively). If a significant correlation was observed, then the relationship between the variable and its predictor was characterized using a separate linear regression.

Correlations between mass-specific mitochondrial properties (OXP I,II, LEAKOmy and CCO per milligram of tissue) of liver and oxidative skeletal muscle were also evaluated using a Pearson's *r* test.

RESULTS

Physical characteristics of stickleback

Animals used for measuring organismal and mitochondrial respiration rates in liver and oxidative skeletal muscle were similar in length and body mass among the temperature groups (length: $F_{2,18}=1.82$, $P=0.19$; mass: $F_{2,23}=2.49$, $P=0.10$) but the condition factor was significantly higher in 12°C animals compared with those at 20°C ($F_{2,22}=8.48$, $P<0.01$) (Table 1). Liver and heart masses did not change with acclimation (data not shown).

The length and body mass of fish used for measuring mitochondrial respiration rate in heart ventricles were higher in the 12°C animals compared with those at 5°C (length: $t_{23}=2.71$, $P<0.05$; mass: $t_{22}=3.59$, $P<0.01$) but the condition factor was equivalent ($t_{22}=0.60$, $P=0.56$) (Table 1).

Stickleback used for enzyme assays had similar condition factors among all three temperature groups ($F_{2,14}=1.08$, $P=0.37$), although the body mass of the 20°C animals was greater than that of the 5°C fish ($F_{2,8}=5.81$, $P<0.01$) and the length of the 20°C fish was greater than that of the 5°C fish ($H_{2,15}=9.59$, $P<0.01$; Table 1).

Aerobic scope

The duration of the experiments did not affect estimates of SMR (5°C: $F_{1,4}=0.11$, $P=0.76$; 12°C: $F_{1,4}=0.05$, $P=0.83$; 20°C: $F_{1,4}=0.97$, $P=0.38$) or MMR (truncated) (5°C: $F_{1,4}=0.86$, $P=0.41$; 12°C: $F_{1,4}=0.58$, $P=0.49$; 20°C: $F_{1,5}=0.92$, $P=0.38$) (Fig. S2).

The truncated MMR estimate was 1.2-fold higher than the traditional MMR estimate for animals at 5°C, but similar for animals at 12 and 20°C (5°C: $t_5=2.61$, $P<0.05$; 12°C: $t_5=1.58$, $P=0.18$; 20°C: $t_6=1.18$, $P=0.28$) (Fig. S3). MMR and AAS estimates are thus reported for the truncated method. SMR and MMR differed among animals in all temperature groups and were highest in animals at 20°C and lowest in animals at 5°C (SMR: $F_{2,15}=251.41$, $P<0.001$; MMR: $F_{2,16}=74.00$, $P<0.001$) (Table S1, Fig. 1A,B). Compared with animals at 5°C, SMR was 1.6- and 3.1-fold higher, and MMR was 2.4- and 4.0-fold higher for animals at 12 and 20°C, respectively. AAS differed among all temperature groups

Table 1. Physical characteristics of threespine stickleback, *Gasterosteus aculeatus*, acclimated to three temperatures

Experiment	Acclimation period	Group	Length (cm)	Body mass (g)	Condition factor
Respirometry (organismal and mitochondrial)	7–20 weeks	5°C	4.88±0.14 (8)	1.32±0.18 (8)	1.13±0.11^{a} (8)
		12°C	5.11±0.40 (10)	1.58±0.40 (10)	1.16±0.13^{a} (10)
		20°C	5.11±0.29 (8)	1.33±0.22 (8)	0.95±0.06^{b} (7)
Mitochondrial respiration in heart ventricles	18–20 weeks	5°C	5.04±0.26* (12)	1.55±0.15* (11)	1.25±0.12 (11)
		12°C	5.32±0.25 (13)	1.84±0.23 (13)	1.22±0.08 (13)
Enzymes assays	21 weeks	5°C	4.65±0.20^{a} (6)	1.28±0.04^{a} (5)	1.30±0.16 (5)
		12°C	5.03±0.23^{a,b} (6)	1.72±0.35^{a,b} (6)	1.34±0.19 (6)
		20°C	5.17±0.26^{b} (6)	1.68±0.20^{b} (6)	1.22±0.08 (6)

Superscript letters indicate significant differences among temperature groups of stickleback within an experiment as identified by a one-way ANOVA followed by Tukey's multiple comparisons test or by a Kruskal–Wallis test followed by a Dunn's multiple comparisons test. Asterisk indicates significant differences between temperature groups within an experiment as identified by Student's *t*-test. Sample sizes are indicated in parentheses. Data are means±s.d.

Journal of Experimental Biology (2022) 225, jeb244659. doi:10.1242/jeb.244659

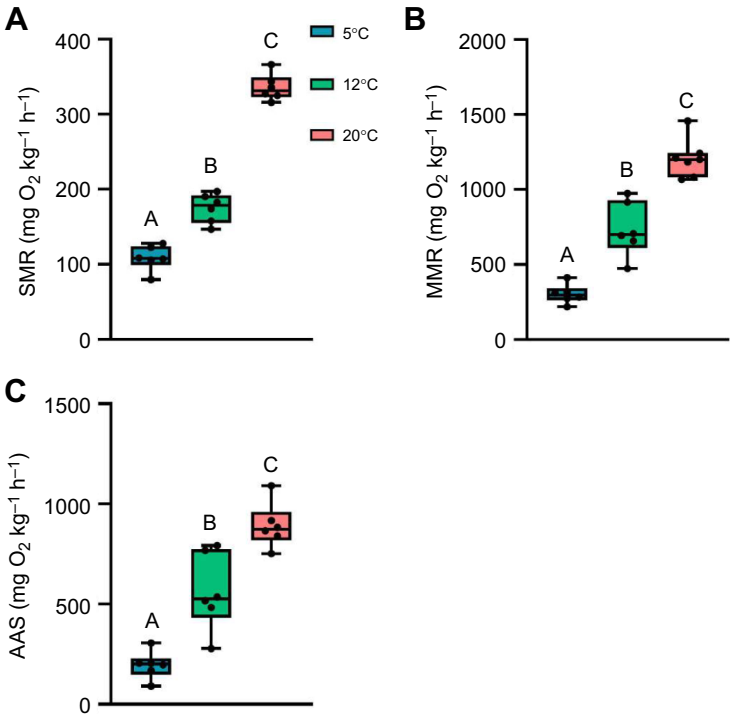

Fig. 1. Metabolic rate and aerobic scope in threespine stickleback, *Gasterosteus aculeatus*, acclimated to three temperatures. (A) Standard metabolic rate (SMR), (B) maximum metabolic rate (MMR) and (C) absolute aerobic scope (AAS). The MMR estimates, and therefore AAS, were calculated using the truncated method (see Materials and Methods for details). Boxes designate quartiles, line designates median and whiskers designate minimum and maximum values (n=6 for all temperature groups except MMR at 20°C, where n=7). Different letters denote significant differences among temperature groups (P<0.05).

($F_{2,15}$=40.11, P<0.001) (Table S1, Fig. 1C). Compared with animals at 5°C, AAS was 2.9- and 4.6-fold higher for animals at 12 and 20°C, respectively.

The Q_{10} for SMR was similar across the acclimation temperatures and ranged from 2.0 (5°C to 12°C) to 2.3 (12°C to 20°C), whereas the Q_{10} for MMR and AAS was higher between 5°C to 12°C (3.5 and 4.5, respectively) than between 12 and 20°C (1.9 and 1.8, respectively) (Table 2).

Mitochondrial respiration

Rates of oxidative phosphorylation supported by complex I (OXP I) and complex I and II (OXP I,II) all increased with acclimation temperature in liver, oxidative skeletal muscle and hearts of sticklebacks (Fig. 2A,B). In liver and oxidative skeletal muscle, rates of OXP I supported flux were 2.2- and 1.5-fold higher, respectively (liver: $F_{2,11}$=7.63, P<0.01; muscle: $F_{2,21}$=3.55, P<0.05), and for OXP I,II, were 3.7- and 1.7-fold higher, respectively, in 20°C-acclimated stickleback compared with stickleback acclimated to 5°C (liver: $F_{2,16}$=58.34, P<0.001; muscle: $F_{2,21}$=5.89, P<0.01) (Fig. 2A,B). Between animals at 5 and 12°C and 12 and 20°C, rates of OXP I supported flux were similar in liver and oxidative muscle but were 2.1-fold higher in hearts of stickleback acclimated to 12°C compared with animals acclimated to 5°C (OXP I: t_8=4.71, P<0.01). Rates of OXP I,II were 1.9-fold higher in liver and 2.5-fold higher in hearts of animals at 12°C compared with those at 5°C, but similar in oxidative muscle (liver: P<0.001; heart: t_7=6.11, P<0.001; muscle: P=0.05) (Fig. 2A,B).

Complex II activity (succinate dehydrogenase) was undetectable in 5 of 6 livers, 5 of 8 oxidative muscles and 4 of 6 hearts of animals acclimated to 5°C, and was significantly higher in liver of stickleback at 20°C compared with livers of fish at 12°C (t_{12}=2.92, P<0.05) (Fig. 2C).

LEAKOmy was significantly higher in liver and muscle of stickleback acclimated to 20°C compared with animals at 5°C (2.8- and 1.6-fold higher, respectively) (liver: $F_{2,13}$=7.54, P<0.01; muscle: $H_{2,21}$=7.98, P<0.05), but equivalent in liver and oxidative muscle mitochondria of stickleback at 5 and 12°C and 12 and 20°C (Fig. 2D). In contrast, LEAKOmy was 1.9-fold higher in hearts of stickleback at 12°C compared with 5°C-acclimated fish (t_{11}=4.57, P<0.001).

Maximal rates of uncoupled respiration (ETS) were significantly higher in liver mitochondria of stickleback acclimated to 20°C compared with stickleback at 5 and 12°C ($F_{2,11}$=11.1, P<0.01)

Table 2. Temperature coefficient (Q_{10}) of metabolic rate and aerobic scope estimates, and mitochondria respiration rates in liver, oxidative skeletal muscle and heart of threespine stickleback, *Gasterosteus aculeatus*, acclimated to three temperatures

Temperature	Component	SMR	MMR	AAS	OXP I	OXPI,II	LEAKOmy	ETS	CCO
5°C to 12°C	Liver	–	–	–	1.8	2.5	3.0	2.1	1.8
	Oxidative skeletal muscle	–	–	–	1.4	1.9	1.4	1.3	1.5
	Heart	–	–	–	2.9	3.7	2.5	2.6	2.5
	Whole animal	2	3.5	4.5	–	–	–	–	–
12°C to 20°C	Liver	–	–	–	1.6	2.2	2.6	1.9	1.7
	Oxidative skeletal muscle	–	–	–	1.4	1.7	1.4	1.2	1.5
	Whole animal	2.3	1.9	1.8	–	–	–	–	–

SMR, standard metabolic rate; MMR, maximum metabolic rate; AAS, absolute aerobic scope; OXP I,II, rate of oxidative phosphorylation supported by complexes I+II; LEAKOmy, rate of leak in the presence of oligomycin; ETS, rate of uncoupled respiration; CCO, uncoupled rate of respiration through cytochrome *c* oxidase (Complex IV). Dash indicates no data.

Journal of Experimental Biology (2022) 225, jeb244659. doi:10.1242/jeb.244659

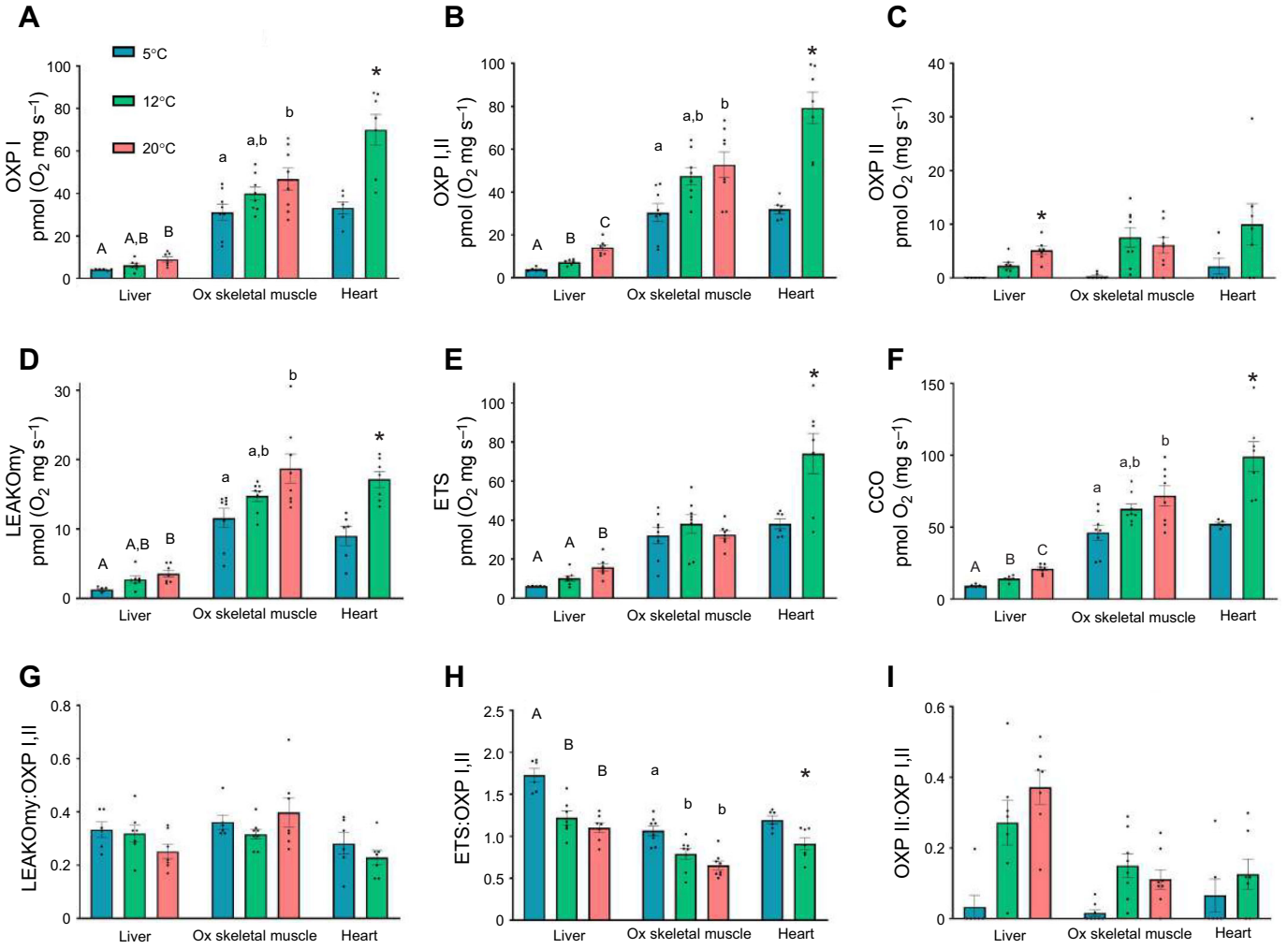

Fig. 2. Mitochondrial properties in permeabilized liver, oxidative (Ox) skeletal muscle and heart ventricle of threespine stickleback, *Gasterosteus aculeatus*, acclimated to three temperatures. (A) Rate of oxidative phosphorylation supported by complex I (OXP I), (B) rate of oxidative phosphorylation supported by complexes I+II (OXP I,II), (C) rate of oxidative phosphorylation through complex II, (D) rate of leak respiration in the presence of oligomycin (LEAKOmy), (E) rate of uncoupled respiration through all complexes (ETS), (F) rate of uncoupled oxidative phosphorylation through cytochrome *c* oxidase (complex IV) (CCO), (G) ratio of oxidative phosphorylation supported by complex I and II to leak respiration in the presence of oligomycin, (H) ratio of uncoupled respiration to oxidative phosphorylation supported by complexes I and II and (I) ratio of oxidative phosphorylation through complex II to oxidative phosphorylation supported by complexes I and II. Data are means±s.e.m., n=5–8. Different letters and asterisks indicate significant differences within each tissue (P<0.05).

(Fig. 2E). In oxidative muscle, ETS rates were similar among all acclimation groups ($F_{2,21}$=0.73, P=0.49). Whereas ETS rates were similar in mitochondria of liver and muscle between 5 and 12°C acclimated stickleback, ETS rates were 1.9-fold higher in mitochondria from hearts of stickleback at 12°C compared with animals at 5°C (t_7=3.40, P<0.05).

The activity of CCO increased with acclimation temperature in liver, oxidative muscle and heart mitochondria. In liver, CCO rates were different among all temperature groups ($F_{2,16}$=40.30, P<0.001) (Fig. 2F). Compared with 5°C-acclimated animals, CCO was 1.5- and 2.3-fold higher in liver of animals acclimated to 12 and 20°C, and 1.5-fold higher in 20°C-acclimated stickleback compared with animals acclimated to 12°C. In oxidative muscle, CCO was equivalent between 5 and 12°C- and 12 and 20°C-acclimated fish, but 1.6-fold higher in stickleback acclimated to 20°C compared with those acclimated to 5°C ($F_{2,21}$=5.74, P<0.05). In heart, CCO was 1.9-fold higher in 12°C-acclimated fish compared with 5°C-acclimated fish (t_6=4.48, P<0.01).

The ratio of LEAKOmy:OXP I,II, a measure of mitochondrial coupling, did not differ among acclimation groups in liver ($F_{2,17}$=2.22, P=0.14) in oxidative skeletal muscle ($H_{2,21}$=3.72, P=0.16) or heart (t_{11}=1.12, P=0.29).

The ratio of ETS:OXP I,II, a measure of reserve capacity in the mitochondrial ETS, was significantly higher in 5°C-acclimated stickleback compared with animals at 12 and 20°C in liver ($F_{2,17}$=19.92, P<0.001) and oxidative skeletal muscle ($F_{2,21}$=13.08, P<0.001), and in hearts, ETS: OXP I,II was significantly higher in stickleback at 5°C than at 12°C (t_{11}=3.21, P<0.01) (Fig. 2H).

When comparing 5 and 12°C animals, the Q_{10} of mitochondrial LEAKOmy, respiration flux supported by complex I (OXP I) and respiration flux through complex I and II (OXP I,II) was 2.5, 2.9 and 3.7 in heart; 3.0, 1.8 and 2.5 in liver; and 1.4, 1.4 and 1.9 in the oxidative skeletal muscle, respectively (Table 2). Between 12 and 20°C, the Q_{10} of mitochondrial respiration rates (OXP I, OXP I,II, LEAKOmy) was between 1.6 and 2.6 in liver and between 1.4 and 1.7 in oxidative skeletal muscle (Table 2). The Q_{10} between 5 and

Journal of Experimental Biology (2022) 225, jeb244659. doi:10.1242/jeb.244659

12°C and between 12 and 20°C was close to 2 in liver and between 1.2 and 1.5 in oxidative muscle for both ETS and CCO (Table 2).

Aerobic and anaerobic metabolic enzymes

The maximal activity of CS was 1.7- and 1.8-fold higher in stickleback at 20°C compared with stickleback at 5 and 12°C in the liver ($F_{2,15}$=14.08, P<0.001) and glycolytic muscle, ($F_{2,15}$=14.57, P<0.001, Fig. 3A,C) respectively. The maximal activity of LDH was significantly higher (2.5-fold) in livers of stickleback at 20°C compared with those at 5 and 12°C ($F_{2,15}$=22.37, P<0.001; Fig. 3D). In contrast, the maximal activities of CS and LDH were equivalent among acclimation groups in oxidative skeletal muscle (CS: $F_{2,15}$=0.93, P=0.42; LDH: $F_{2,15}$=2.23, P=0.14; Fig. 3B,E).

Relationship between mitochondrial function and aerobic scope

SMR, MMR and mitochondrial function in liver and oxidative pectoral muscle were measured in the same individuals, providing an opportunity to explore the relationship between mitochondrial function and $\dot{M}_{O_2}$. A PCA was performed to explore whether rates of OXP I,II, LEAKOmy, ETS and CCO were associated with SMR and MMR (Fig. S4). Most of the variation in these parameters was explained by components 1 (Dim1) and 2 (Dim2) of the PCA analysis (48.9% and 20.8%, respectively). SMR and MMR were grouped together within the same quadrant, indicating they were positively correlated, with a quality of representation on the factor map of 0.79 and 0.73, respectively. Several mitochondrial properties of the liver, including OXP I,II and ETS, were in the same quadrant as SMR and MMR.

Absolute SMR was positively correlated with CCO activity in both liver and oxidative muscle (liver: r=0.75, P<0.01; muscle: r=0.51, P<0.05, respectively) (Table 3), and absolute MMR was positively correlated with liver CCO activity (r=0.76, P<0.001) (Table 4). Significant, positive relationships were also observed between absolute SMR and liver CCO activity (r^2=0.56, P<0.01) (Fig. 4A), between absolute SMR and oxidative muscle CCO activity (r^2=0.26, P<0.05) (Fig. 4B), and between absolute MMR and liver CCO activity (r^2=0.57, P<0.001) (Fig. 4C).

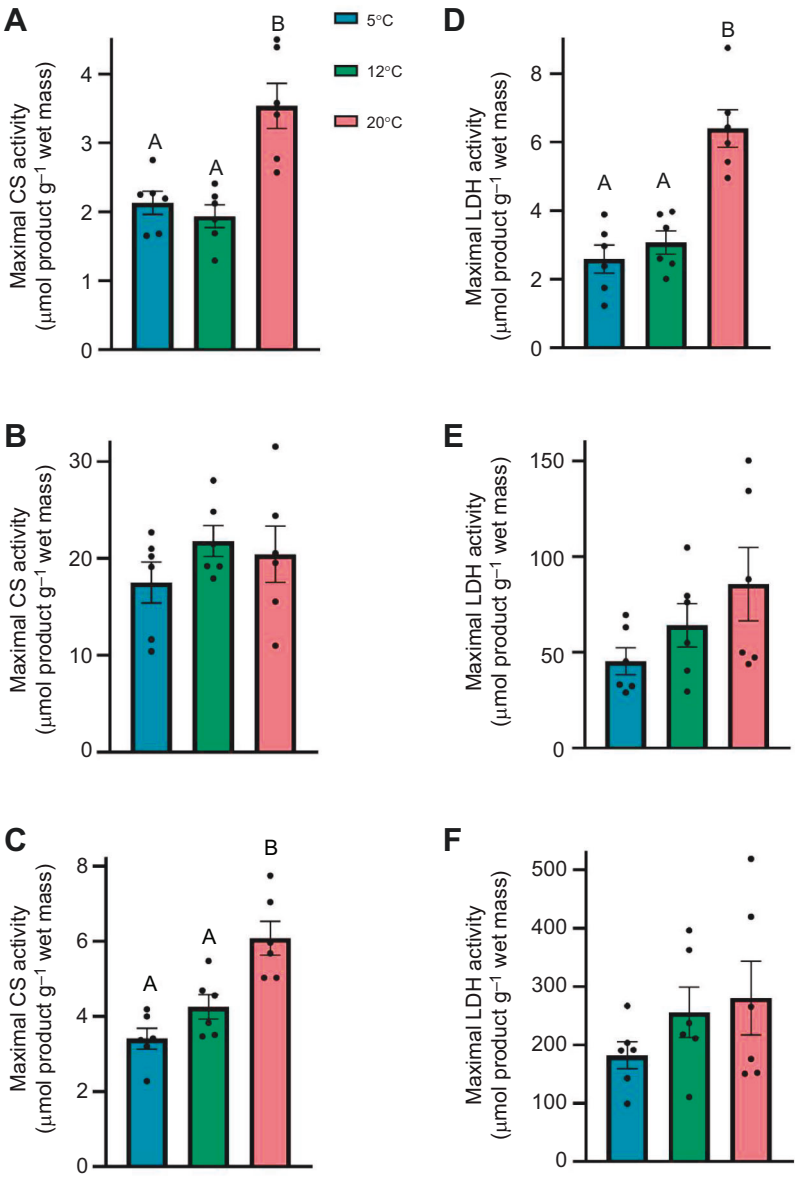

Fig. 3. Maximal activity of citrate synthase (CS) and lactate dehydrogenase (LDH) in tissues of threespine stickleback, *Gasterosteus aculeatus*, acclimated to three temperatures. (A,D) Liver, (B,E) oxidative skeletal muscle and (C,F) glycolytic skeletal muscle. Data are means±s.e.m., n=6 for each temperature group. Different letters denote significant differences among temperature groups (P<0.05).

Journal of Experimental Biology (2022) 225, jeb244659. doi:10.1242/jeb.244659

Table 3. Results from correlation analyses of absolute standard metabolic rate (Abs SMR) and mitochondrial properties [phosphorylation respiration rate (OXP I,II, log) and leak respiration rate (LEAKOmy) normalized to the activity of complex IV (CCO)] in liver and oxidative skeletal muscle (OxM) of threespine stickleback, *Gasterosteus aculeatus*, acclimated to three temperatures

	Abs SMR	Temperature (°C)	Mass	Liver log OXP I,II/CCO	Liver LEAKOmy/CCO	Liver CCO	OxM OXP I,II/CCO	OxM LEAKOmy/CCO	OxM CCO
Abs SMR		<0.001*	0.60	0.44	0.46	**<0.01***	0.05	0.67	**0.03***
Temperature (°C)	**0.89**		0.42	0.11	0.27	<0.001*	0.06	0.20	0.04*
Mass	0.13	−0.20		0.01*	0.73	0.14	0.68	0.46	0.58
Liver log OXP I,II/CCO	−0.22	−0.42	0.65		0.28	0.01*	0.86		
Liver LEAKOmy/CCO	0.21	0.29	−0.10	0.29		0.39		0.46	
Liver CCO	**0.75**	0.92	−0.39	−0.63	0.23				0.14
OxM OXP I,II/CCO	−0.47	−0.45	0.10	0.05				0.92	<0.001*
OxM LEAKOmy/CCO	0.11	0.30	−0.18		0.20		0.03		0.59
OxM CCO	**0.51**	0.48	−0.13			0.39	−0.94	−0.13	

Pearson's *r* coefficients are shown in the lower half of the table and *P*-values are shown at the top. Asterisks highlight significant *P*-values. Values in bold highlight a significant correlation of absolute SMR with the corresponding mitochondrial property.

Mass-specific mitochondrial capacities for OXP I,II, LEAKOmy and CCO were not correlated between liver and oxidative muscle at any acclimation temperature (P>0.05; Table S2).

DISCUSSION

Results from this study contribute to our understanding of the plasticity and limits of thermal acclimation of fishes. SMR, MMR and AAS all increased with acclimation temperature along with mitochondrial oxidative phosphorylation rates in liver, oxidative skeletal muscle and hearts of stickleback. Some aspects of cellular metabolism were similar among temperature groups in oxidative skeletal muscle but not liver (e.g. CS and LDH activity, uncoupled respiration rates), glycolytic skeletal muscle (e.g. CS and LDH activity) or cardiac muscle (e.g. uncoupled respiration rates), suggesting greater thermal compensation in pectoral muscle, possibly owing to its importance in the labriform swimming style of stickleback that is used to maintain position in the water column. In both liver and oxidative skeletal muscle, SMR was positively correlated with CCO activity, and MMR was positively correlated with CCO activity in the liver, reflecting the central role of CCO in fine-tuning and regulating cellular metabolism (Little et al., 2018). Notably, however, mitochondrial respiration rates were not correlated between liver and oxidative skeletal muscle, further highlighting tissue- and organ-specific differences in mitochondrial remodeling in response to temperature. Overall, these results indicate that AAS and mitochondrial function are highly influenced by environmental temperature, and that CCO activity in liver plays a central role in setting organismal $\dot{M}_{O_2}$.

Aerobic scope increases with acclimation temperature

SMR, MMR and AAS all increased with acclimation temperature in stickleback, similar to results reported for other eurythermal marine and freshwater fish species, such as juvenile European sea bass acclimated to 7–30°C (Claireaux et al., 2006) and killifish (*Fundulus heteroclitus*) acclimated to 5–30°C (Healy and Schulte, 2012). Between 5 and 12°C, MMR increased more than SMR in stickleback, with MMR increasing 2.4-fold and SMR increasing only 1.6-fold. In contrast, between 12 and 20°C, SMR and MMR increased similarly, with MMR increasing 1.6-fold and SMR increasing 1.9-fold. AAS was highest in stickleback at 20°C, which is near the upper seasonal temperature range of this population,

Table 4. Results from correlation analyses of absolute maximum metabolic rate (Abs MMR) calculated using the truncated method and mitochondrial properties [phosphorylation respiration rate (OXP I,II, log) and leak respiration rate (LEAKOmy) normalized to the activity of complex IV (CCO)] in liver and oxidative skeletal muscle (OxM) of threespine stickleback, *Gasterosteus aculeatus*, acclimated to three temperatures

	Abs MMR truncated	Temperature (°C)	Mass	Liver log OXP I,II/CCO	Liver LEAKOmy/CCO	Liver CCO	OxM log OXP I,II/CCO	OxM LEAKOmy/CCO	OxM CCO
Abs MMR truncated		<0.001*	0.27	0.51	0.59	**<0.001***	0.11	0.41	0.14
Temperature (°C)	**0.86**		0.42	0.11	0.27	<0.001*	0.06	0.20	0.04*
Mass	0.27	−0.20		0.01	0.73	0.14	0.68	0.46	0.58
Liver log OXP I,II/CCO	−0.18	−0.42	−0.06		0.28	0.01*	0.86		
Liver LEAKOmy/CCO	0.14	0.29	−0.10	0.29		0.39		0.13	
Liver CCO	**0.76**	0.92	−0.39	−0.63	0.23				0.14
OxM log OXP I,II/CCO	−0.37	−0.45	0.10	0.05				0.21	0.99
OxM LEAKOmy/CCO	0.20	0.30	−0.218		0.20		0.03		0.70
OxM CCO	0.35	0.48	−0.13			0.39	−0.94	−0.13	

Pearson's *r* coefficients are shown in the lower half of the table and *P*-values are shown at the top. Asterisks highlight significant *P*-values. Values in bold highlight significant correlation of absolute MMR with the corresponding mitochondrial property.

Journal of Experimental Biology (2022) 225, jeb244659. doi:10.1242/jeb.244659

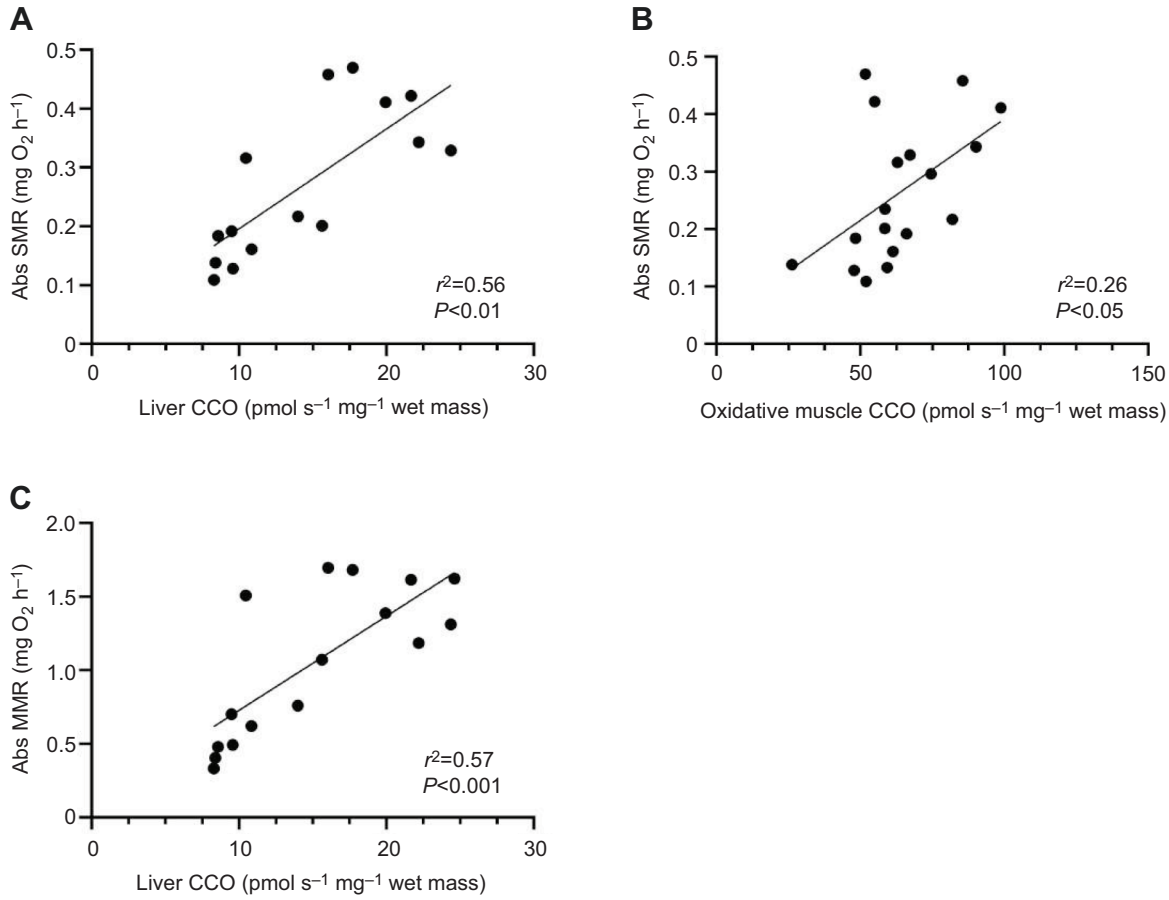

Fig. 4. Relationship between absolute (Abs) metabolic rate and cytochrome *c* oxidase (CCO) activity of threespine stickleback, *Gasterosteus aculeatus*, acclimated to three temperatures. (A) Relationship between absolute standard metabolic rate (Abs SMR) and CCO in liver. (B) Relationship between Abs SMR and CCO in oxidative muscle. (C) Relationship between absolute maximum metabolic rate (Abs MMR) and CCO in liver. n=15, 18 and 16 for A, B and C, respectively.

although studies in other fishes suggest the temperature at which AAS is highest does not necessarily reflect an optimal temperature for all physiological processes. For example, in killifish acclimated to temperatures between 5 and 35°C, AAS is maximal at 25°C for both northern and southern populations of killifish, yet growth rate is negative at 25 and 30°C (Fangue et al., 2009), and gonadosomatic index is highest in 10°C-acclimated females from the northern population (Healy and Schulte, 2012). In pink salmon (*Oncorhynchus gorbuscha*), T_{opt} of AAS is 21°C but cardiac output declines above 17°C (Clark et al., 2011), and in Atlantic halibut (*Hippoglossus hippoglossus*), AAS increases with acclimation temperature up to 16°C but specific growth rate declines above 14°C (Gräns et al., 2014). Together, these data suggest that maximal AAS does not necessarily reflect an optimum temperature, as described by the multiple performance-multiple optima hypothesis, which asserts that each physiological process has a specific thermal optimum (Clark et al., 2013).

The low AAS of stickleback acclimated to 5°C is consistent with our previous study of an Alaskan freshwater stickleback population (Ressel et al., 2022). The AAS at 5°C is equivalent between the two populations ($F_{1,30}$=3.48, P=0.07) and AAS increases with acclimation temperature in both (Ressel et al., 2022). Low SMR and MMR have also been observed in several populations of cold-acclimated (6°C) ninespine stickleback (*Pungitius pungitius*) (Bruneaux et al., 2014). It is conceivable that stickleback undergo winter dormancy, as has been described for other fishes (Crawshaw, 1984; Reeve et al., 2022). The higher Q_{10} values for MMR between 5 and 12°C (3.5) compared with Q_{10} values between 12 and 20°C (1.9) (Table 2) also suggest a lower degree of thermal compensation at colder temperatures compared with warmer ones, although without measuring SMR and MMR in response to an acute temperature exposure, we cannot be certain.

Mitochondrial function is altered by temperature acclimation

Rates of phosphorylating respiration supported by complexes I and II (OXP I,II) increased with acclimation temperature in liver, oxidative skeletal muscle and hearts (Fig. 2B), as did rates of uncoupled respiration (ETS) in liver and heart (Fig. 2E). Rates of phosphorylating respiration (OXP I,II) increased to the greatest extent in hearts between 5 and 12°C (2.5-fold) compared with oxidative muscle (1.6-fold) and liver (1.9-fold) (Fig. 2B), paralleling a large increase in MMR between 5 and 12°C (2.4-fold) and providing support for the supposition that cardiac aerobic capacity plays a central role in setting MMR (Ekström et al., 2017; Pichaud et al., 2017; Ressel et al., 2022).

Although OXP I,II is low at 5°C in stickleback, there is a high ETS reserve capacity reflected in the higher ratio of ETS:OXP I,II in liver, oxidative skeletal muscle and hearts of 5°C-acclimated stickleback compared with 12°C- and 20°C-acclimated fishes

(Fig. 2H), suggesting that although cellular respiration may be suppressed at low temperature, it is capable of increasing when needed.

Complex II activity (OXP II; succinate dehydrogenase) and OXP II:OXP I,II increased with acclimation temperature in liver and oxidative skeletal muscle (Fig. 2C,I). At 5°C, complex II activity was undetectable in liver, oxidative muscle and hearts of most stickleback. Similarly, in mammalian brain mitochondria, complex II activity declines to a greater extent than complex I with a decrease in temperature from 37°C to 28°C (Pamenter et al., 2018). The increase in succinate-fueled respiration in response to an increase in acclimation temperature may be beneficial for maintaining mitochondrial function at elevated temperature, as complex II seems more resilient at high temperatures compared with complex I in some fishes (Michaelsen et al., 2021). In rainbow trout acclimated to 16°C, complex I activity in cardiac mitochondria deteriorated at temperatures above 20°C, whereas complex II activity did not, and rather, continued to increase with assay temperature up to the maximum temperature assayed (30°C) (Michaelsen et al., 2021). Similarly, in killifish, mitochondrial respiration rates were depressed in animals acclimated to high temperature (33°C) owing to a decrease in the activity of complex I (Chung and Schulte, 2015). Interestingly, complex II displays an Arrhenius breakpoint at 10°C in rainbow trout, suggesting that it is less stable at cold temperatures (Michaelsen et al., 2021). The differences in thermal stability of complex I and II may be attributable to changes in membrane composition, especially cardiolipin, a critical annular lipid surrounding and stabilizing complex I (Jussupow et al., 2019). The greater reliance on complex I activity at colder temperatures likely improves the efficiency of ATP synthesis because complex I, unlike complex II, is a proton pump, directly contributing to the proton motive force used to synthesize ATP. Greater efficiency in ATP synthesis may be important in winter, when food may be scarce. Interestingly, complex II is inhibited during hibernation in liver and skeletal muscle mitochondria of thirteen-lined ground squirrels (*Ictidomys tridecemlineatus*), contributing to metabolic suppression (Brown and Staples, 2014; Brown et al., 2013). Thus, it is conceivable that low complex II activity at 5°C may contribute to the low $\dot{M}_{O_2}$ of stickleback at 5°C.

Overall, the proportion of succinate-fueled phosphorylating respiration is higher in liver than in heart and oxidative skeletal muscle (Fig. 2I). Similar differences have been observed in mammalian mitochondria (Kappler et al., 2019). Combined proteomic and mitochondrial function assays in mice and humans indicate that liver mitochondria rely more on succinate to fuel respiration and utilize complex I substrates for gluconeogenesis and ketogenesis, whereas muscle has a higher rate of respiration on complex I substrates than liver (Kappler et al., 2019). Our data suggest the same may be true for fishes.

LEAKOmy increased with acclimation temperature in all tissues, but the proportion of LEAKOmy relative to OXP I,II was equivalent among all temperature groups (Fig. 2G). When compared using a two-way ANOVA, at 5 and 12°C, OXP I,II: LEAKOmy was higher in hearts than in liver and muscle, indicative of a higher degree of coupling in cardiac mitochondria ($F_{2,36}$=6.34, P<0.01). Mitochondrial proton leak is influenced by the surface area of inner membrane, phospholipid fatty acid composition (Porter et al., 1996) and uncoupling proteins (Jastroch et al., 2005; Nicholls, 2021). For many fish species, mitochondrial proton leak increases in response to an acute increase in temperature (Iftikar and Hickey, 2013; Michaelsen et al., 2021; Pichaud et al., 2017), and in cardiac mitochondria, an increase in leak is associated with loss of cardiac function (Iftikar and Hickey, 2013; O'Brien et al., 2018). Results presented here suggest that acclimation may minimize mitochondrial membrane leakiness at elevated temperature, consistent with a previous study in rainbow trout (*Oncorhynchus mykiss*), where acute warming from 10°C to 16°C increases proton leak, but then declines by day 2 of acclimation to 16°C (Pichaud et al., 2017). The resiliency of mitochondrial proton leakage in stickleback may contribute to their high thermal tolerance, broad distribution and high critical thermal maximum, which, for a population of marine stickleback at the far northern end of their distribution on the North Slope of Alaska, is a remarkably high 30.7°C (Bilyk and Sformo, 2021). Interestingly, a recent study investigating thermal tolerance and predicted range change owing to climate change determined that evolution of cold tolerance has a greater impact on predicted range changes than heat tolerance for stickleback (Wuitchik et al., 2022).

Studies quantifying metabolic enzyme activity and/or mitochondrial function in response to temperature acclimation in fishes have shown that, in general, enzyme activity (and enzyme concentration) per gram tissue increases in response to cold acclimation to offset the thermodynamic effects of cold temperature on the catalytic rate of enzymes (Guderley, 1990; Guderley et al., 2001; Johnston and Dunn, 1987; Kleckner and Sidell, 1985; Vézina and Guderley, 1991). A previous study in stickleback determined that the activities of both CS and CCO are higher in liver and oxidative skeletal muscle of cold-acclimated stickleback (8°C) compared with warm-acclimated fishes (20°C) when measured at a common temperature (Orczewska et al., 2010). Nevertheless, results from the present study indicate that despite the increase in CS and CCO activity per gram tissue and mitochondrial density with cold acclimation, the activity of metabolic enzymes and rates of mitochondrial respiration decrease with a decrease in acclimation temperature in several organs and tissues, even after approximately 5 months of acclimation.

Temperature-induced metabolic remodeling differs among tissues

Although, in general, mitochondrial respiration rates increase with acclimation temperature in all tissues examined, the lack of correlation in mitochondrial respiration states between liver and oxidative muscle suggests differences in their response to temperature (Table S2). Additionally, mitochondrial respiration rates increased to a greater extent in hearts compared with liver and oxidative skeletal muscle between 5 and 12°C. Active metabolic compensation is suggested to occur when Q_{10}<2 (Song et al., 2019). Given this, our data suggest that the greatest thermal compensation occurred in oxidative skeletal muscle, which displayed the lowest Q_{10} for values for mitochondrial function (Table 2) and equivalent rates of ETS (Fig. 2E) and activities of LDH and CS among all acclimation groups (Fig. 3B,E). Because stickleback, as labriform swimmers, use their pectoral adductor and abductor muscles to move their pectoral fins in a rowing motion to maintain their position in the water column (Whoriskey and Wootton, 1987), maintaining ATP production in the pectoral adductor muscle may be crucial for maintaining swimming performance across a range of habitat temperatures.

SMR and MMR are associated with CCO activity

Rates of oxidative phosphorylation (OXP I,II) increased with acclimation temperature in liver, oxidative skeletal muscle and heart, paralleling increases in SMR and MMR. This contrasts with triplefin fish, where SMR increased with acclimation temperature

between 18 and 24°C but phosphorylating respiration rates and leak rates of fast glycolytic muscle fibers were equivalent between fish acclimated to 18 and 24°C (Khan et al., 2014). These differences may be due to tissue-specific differences in mitochondrial thermal plasticity. Mitochondrial function was also unaffected by temperature acclimation in the glycolytic muscle of southern catfish (*S. meridionalis*) in contrast to the heart and liver, which displayed higher mitochondrial oxidative capacities in fish acclimated to 12.5°C compared with fish acclimated to 27.5°C when measured at temperatures between 12.5°C and 27.5°C (Yan and Xie, 2015).

Although PCA suggested an association between OXP I,II and SMR and MMR (Fig. S4), there was not a significant correlation between OXP I,II and SMR or MMR when OXP I,II was normalized to CCO activity (Tables 3 and 4). Rather, SMR was correlated with CCO activity in liver and oxidative skeletal muscle, and MMR was correlated with CCO activity in the liver. This is consistent with a study in brown trout (*Salmo trutta*), where SMR and MMR estimates are positively correlated with CCO activity in liver (Norin and Malte, 2012). The liver accounts for a large proportion of the oxygen consumed to support SMR in mammals (Rolfe and Brown, 1997), and likely in fish as well. The correlation between CCO activity and MMR in liver is not as easily reconciled, although as noted by Garland (1984) and cited by Norin and Malte (2012), the correlation between MMR and oxidative capacity of the liver may be due to the liver's role in oxidizing lactate and/or gluconeogenesis during post-exercise recovery. In total, these data indicate that temperature-induced metabolic remodeling in liver contributes significantly to adjustments in SMR and MMR in stickleback.

Although mitochondrial proton leak comprises ∼20% of oxygen consumed in liver (Porter et al., 1996) and is positively correlated with SMR in a variety of ectotherms and endotherms (Brookes et al., 1998), we did not observe a correlation between LEAKOmy and SMR. This contrasts with results from an intraspecific study of brown trout, which found a positive correlation between mitochondrial leak respiration in liver and SMR, as well as between mitochondrial leak respiration in glycolytic muscle and MMR (Salin et al., 2016). In stickleback, the relative proportion of leak respiration (LEAKOmy) to OXP I,II was not altered by temperature acclimation in liver, oxidative skeletal muscle or heart. Conceivably by minimizing proton leak at high temperature, more energy can be allocated to support traits that might maintain a high AAS (cardiac output, lactate oxidation in liver) and fitness.

The central role of CCO in setting metabolic rate is interesting given the complicated nature of its synthesis. CCO is composed of 13 subunits, three of which form the catalytic core encoded in the mitochondrial genome; the other 10 subunits, several of which have paralogs, are encoded in the nuclear genome (Little et al., 2018). Thus, any alteration in CCO synthesis in response to temperature requires coordination between the two genomes. Interestingly, the expression of the nuclear-encoded CCO subunits (and paralogs) does not change in a coordinated fashion in response to temperature acclimation in fish; rather, the expression of some subunits and paralogs increases more than others in response to cold acclimation, suggesting there may be temperature-specific paralogs (Duggan et al., 2011). Moreover, some of the CCO subunits have tissue-specific isoforms, permitting tissue-specific fine-tuning of cellular metabolism (Kadenbach et al., 2000). Thus, it is conceivable that changes in the expression of one or few CCO subunits in response to temperature may permit adjustments in mitochondrial function without changes in mitochondrial abundance, as has been observed in stickleback (Orczewska et al., 2010), contributing to tissue-specific metabolic remodeling and playing a key role in the metabolic thermal plasticity of fishes.

Competing interests

The authors declare no competing or financial interests.

Author contributions

Conceptualization: K.M.O.; Methodology: L.C., K.N.R., A.A.B., P.M., E.C.R.-G., K.M.O.; Software: L.C., K.N.R., A.A.B.; Validation: L.C., K.N.R., K.M.O.; Formal analysis: L.C., K.N.R., A.A.B., P.M., E.C.R.-G., K.M.O.; Investigation: K.N.R., E.C.R.-G., P.M., A.A.B., K.M.O.; Resources: K.M.O.; Data curation: L.C., K.N.R., A.A.B., P.M., E.C.R.-G., K.M.O.; Writing - original draft: L.C., K.N.R., A.A.B., P.M., E.C.R.-G., K.M.O.; Writing - review & editing: L.C., K.N.R., K.M.O.; Visualization: L.C., K.M.O.; Supervision: K.M.O.; Project administration: K.M.O.; Funding acquisition: K.M.O.

Funding

Funding was provided by a grant from the National Science Foundation (IOS 1756191 to K.M.O.) and an Institutional Development Award (IDeA) from the National Institute of General Medical Sciences of the National Institutes of Health (NIH) under grant number P20GM103395. The content is solely the responsibility of the authors and does not necessarily reflect the official views of the NIH. Deposited in PMC for release after 12 months.

Data availability

Data are available from Dryad at (Cominassi et al., 2022): doi:10.5061/dryad.hdr7sqvmw

References

Bilyk, K. T. and Sformo, T. L. (2021). Varying heat tolerance among Arctic nearshore fishes. *Polar Biol.* **44**, 607-612. doi:10.1007/s00300-021-02815-6

Brookes, P. S., Buckingham, J. A., Tenreiro, A. M., Hulbert, A. J. and Brand, M. D. (1998). The proton permeability of the inner membrane of liver mitochondria from ectothermic and endothermic vertebrates and from obese rats: correlations with standard metabolic rate and phospholipid fatty acid composition. *Comp. Biochem. Physiol. B Biochem. Mol. Biol.* **119**, 325-334. doi:10.1016/S0305-0491(97)00357-X

Brown, J. C. L. and Staples, J. F. (2014). Substrate-specific changes in mitochondrial respiration in skeletal and cardiac muscle of hibernating thirteen-lined ground squirrels. *J. Comp. Physiol. B Biochem. Syst. Environ. Physiol.* **184**, 401-414. doi:10.1007/s00360-013-0799-3

Brown, J. C. L., Chung, D. J., Cooper, A. N. and Staples, J. F. (2013). Regulation of succinate-fuelled mitochondrial respiration in liver and skeletal muscle of hibernating thirteen-lined ground squirrels. *J. Exp. Biol.* **216**, 1736-1743. doi:10.1242/jeb.078519

Brownscombe, J. W., Cooke, S. J., Algera, D. A., Hanson, K. C., Eliason, E. J., Burnett, N. J., Danylchuk, A. J., Hinch, S. G. and Farrell, A. P. (2017). Ecology of exercise in wild fish: integrating concepts of individual physiological capacity, behavior, and fitness through diverse case studies. *Integr. Comp. Biol.* **57**, 281-292. doi:10.1093/icb/icx012

Bruneaux, M., Nikinmaa, M., Laine, V. N., Lindström, K., Primmer, C. R. and Vasemägi, A. (2014). Differences in the metabolic response to temperature acclimation in nine-spined stickleback (*Pungitius pungitius*) populations from contrasting thermal environments. *J. Exp. Zool. A Ecol. Genet. Physiol.* **321**, 550-565. doi:10.1002/jez.1889

Chabot, D., McKenzie, D. J. and Craig, J. F. (2016a). Metabolic rate in fishes: definitions, methods and significance for conservation physiology. *J. Fish Biol.* **88**, 1-9. doi:10.1111/jfb.12873

Chabot, D., Steffensen, J. F. and Farrell, A. P. (2016b). The determination of standard metabolic rate in fishes. *J. Fish Biol.* **88**, 81-121. doi:10.1111/jfb.12845

Chabot, D., Zhang, Y. and Farrell, A. P. (2021). Valid oxygen uptake measurements: using high r^2 values with good intentions can bias upward the determination of standard metabolic rate. *J. Fish Biol.* **98**, 1206-1216. doi:10.1111/jfb.14650

Chung, D. J. and Schulte, P. M. (2015). Mechanisms and costs of mitochondrial thermal acclimation in a eurythermal killifish (*Fundulus heteroclitus*). *J. Exp. Biol.* **218**, 1621-1631. doi:10.1242/jeb.120444

Chung, D. J., Bryant, H. J. and Schulte, P. M. (2017). Thermal acclimation and subspecies-specific effects on heart and brain mitochondrial performance in a eurythermal teleost (*Fundulus heteroclitus*). *J. Exp. Biol.* **220**, 1459-1471. doi:10.1242/jeb.151217

Claireaux, G., Couturier, C. and Groison, A.-L. (2006). Effect of temperature on maximum swimming speed and cost of transport in juvenile European sea bass (*Dicentrarchus labrax*). *J. Exp. Biol.* **209**, 3420-3428. doi:10.1242/jeb.02346

Clark, T. D., Jeffries, K. M., Hinch, S. G. and Farrell, A. P. (2011). Exceptional aerobic scope and cardiovascular performance of pink salmon (*Oncorhynchus gorbuscha*) may underlie resilience in a warming climate. *J. Exp. Biol.* **214**, 3074-3081. doi:10.1242/jeb.060517

Clark, T. D., Sandblom, E. and Jutfelt, F. (2013). Aerobic scope measurements of fishes in an era of climate change: Respirometry, relevance and recommendations. *J. Exp. Biol.* **216**, 2771-2782. doi:10.1242/jeb.084251
Clarke, A. and Johnston, N. M. (1999). Scaling of metabolic rate with body mass and temperature in teleost fish. *J. Anim. Ecol.* **68**, 893-905. doi:10.1046/j.1365-2656.1999.00337.x
Cominassi, L., Ressel, K. N., Brooking, A. A., Marbacher, P., Ransdell-Green, E. C. and O'Brien, K. M. (2022). Metabolic rate increases with thermal acclimation and is associated with mitochondrial function in some tissues of threespine stickleback. Dryad, Dataset, doi:10.5061/dryad.hdr7sqvmw
Crawshaw, L. I. (1984). Low-temperature dormancy in fish. *Am. J. Physiol. Regul. Integr. Comp. Physiol.* **15**, R479-R486. doi:10.1152/ajpregu.1984.246.4.R479
Doerrier, C., Garcia-Souza, L. F., Krumschnabel, G., Wohlfarter, Y., Mészáros, A. T. and Gnaiger, E. (2018). High-resolution FluoRespirometry and OXPHOS protocols for human cells, permeabilized fibers from small biopsies of muscle, and isolated mitochondria. *Methods Mol. Biol.* **1782**, 31-70. doi:10.1007/978-1-4939-7831-1_3
Duggan, A. T., Kocha, K. M., Monk, C. T., Bremer, K. and Moyes, C. D. (2011). Coordination of cytochrome c oxidase gene expression in the remodelling of skeletal muscle. *J. Exp. Biol.* **214**, 1880-1887. doi:10.1242/jeb.053322
Egginton, S. and Sidell, B. D. (1989). Thermal acclimation induces adaptive changes in subcellular structure of fish skeletal muscle. *Am. J. Physiol. Regul. Integr. Comp. Physiol.* **256**, R1-R9. doi:10.1152/ajpregu.1989.256.1.R1
Ekström, A., Sandblom, E., Blier, P. U., Cyr, B.-A. D., Brijs, J. and Pichaud, N. (2017). Thermal sensitivity and phenotypic plasticity of cardiac mitochondrial metabolism in European perch, *Perca fluviatilis*. *J. Exp. Biol.* **220**, 386-396. doi:10.1242/jeb.150698
Fangue, N. A., Mandic, M., Richards, J. G. and Schulte, P. M. (2008). Swimming performance and energetics as a function of temperature in killifish *Fundulus heteroclitus*. *Physiol. Biochem. Zool.* **81**, 389-401. doi:10.1086/589109
Fangue, N. A., Richards, J. G. and Schulte, P. M. (2009). Do mitochondrial properties explain intraspecific variation in thermal tolerance? *J. Exp. Biol.* **212**, 514-522. doi:10.1242/jeb.024034
Farrell, A. P., Eliason, E. J., Sandblom, E. and Clark, T. D. (2009). Fish cardiorespiratory physiology in an era of climate change. *Can. J. Zool.* **87**, 835-851. doi:10.1139/Z09-092
Ferreira, E. O., Anttila, K. and Farrell, A. P. (2014). Thermal optima and tolerance in the eurythermic goldfish (*Carassius auratus*): relationships between whole-animal aerobic capacity and maximum heart rate. *Physiol. Biochem. Zool.* **87**, 599-611. doi:10.1086/677317
Garland, T., Jr (1984). Physiological correlates of locomotory performance in a lizard: an allometric approach. *Am. J. Physiol. Regul. Integr. Comp. Physiol.* **16**, 806-815. doi:10.1152/ajpregu.1984.247.5.R806
Gräns, A., Jutfelt, F., Sandblom, E., Jönsson, E., Wiklander, K., Seth, H., Olsson, C., Dupont, S., Ortega-Martinez, O., Einarsdottir, I. et al. (2014). Aerobic scope fails to explain the detrimental effects on growth resulting from warming and elevated CO_2 in Atlantic halibut. *J. Exp. Biol.* **217**, 711-717. doi:10.1242/jeb.096743
Guderley, H. (1990). Functional significance of metabolic responses to thermal acclimation in fish muscle. *Am. J. Physiol. Regul. Integr. Comp. Physiol.* **259**, R245-R252. doi:10.1152/ajpregu.1990.259.2.R245
Guderley, H., Leroy, P. H. and Gagné, A. (2001). Thermal acclimation, growth, and burst swimming of threespine stickleback: enzymatic correlates and influence of photoperiod. *Physiol. Biochem. Zool.* **74**, 66-74. doi:10.1086/319313
Hansen, C. A. and Sidell, B. D. (1983). Atlantic hagfish cardiac muscle: metabolic basis of tolerance to anoxia. *Am. J. Physiol. Regul. Integr. Comp. Physiol.* **13**, R356-R362. doi:10.1152/ajpregu.1983.244.3.R356
Healy, T. M. and Schulte, P. M. (2012). Thermal acclimation is not necessary to maintain a wide thermal breadth of aerobic scope in the common killifish (*Fundulus heteroclitus*). *Physiol. Biochem. Zool.* **85**, 107-119. doi:10.1086/664584
Hvas, M., Folkedal, O., Imsland, A. and Oppedal, F. (2017). The effect of thermal acclimation on aerobic scope & critical swimming speed in Atlantic salmon, *Salmo salar*. *J. Exp. Biol.* **220**, 2757-2764. doi:10.1242/jeb.154021
Iftikar, F. I. and Hickey, A. J. R. (2013). Do mitochondria limit hot fish hearts? Understanding the role of mitochondrial function with heat stress in *Notolabrus celidotus*. *PLoS ONE* **8**, e64120. doi:10.1371/journal.pone.0064120
Iftikar, F. I., MacDonald, J. R., Baker, D. W., Renshaw, G. M. C. and Hickey, A. J. R. (2014). Could thermal sensitivity of mitochondria determine species distribution in a changing climate? *J. Exp. Biol.* **217**, 2348-2357. doi:10.1242/jeb.098798
Jastroch, M., Wuertz, S., Kloas, W. and Klingenspor, M. (2005). Uncoupling protein 1 in fish uncovers an ancient evolutionary history of mammalian nonshivering thermogenesis. *Physiol. Genomics* **22**, 150-156. doi:10.1152/physiolgenomics.00070.2005
Johnston, I. A. and Dunn, J. (1987). Temperature acclimation and metabolism in ectotherms with particular reference to teleost fish. *Symp. Soc. Exp. Biol.* **41**, 67-93.
Jussupow, A., Di Luca, A. and Kaila, V. R. I. (2019). How cardiolipin modulates the dynamics of respiratory complex I. *Sci. Adv.* **5**, 1-8. doi:10.1126/sciadv.aav1850
Kadenbach, B., Hüttemann, M., Arnold, S., Lee, I. and Bender, E. (2000). Mitochondrial energy metabolism is regulated via nuclear-coded subunits of cytochrome *c* oxidase. *Free Rad. Biol. Med.* **29**, 211-221. doi:10.1016/S0891-5849(00)00305-1
Kappler, L., Hoene, M., Hu, C., von Toerne, C., Li, J., Bleher, D., Hoffmann, C., Böhm, A., Kollipara, L., Zischka, H. et al. (2019). Linking bioenergetic function of mitochondria to tissue-specific molecular fingerprints. *Am. J. Physiol. Endocrinol. Metab.* **317**, E374-E387. doi:10.1152/ajpendo.00088.2019
Khan, J. R., Iftikar, F. I., Herbert, N. A., Gnaiger, E. and Hickey, A. J. R. (2014). Thermal plasticity of skeletal muscle mitochondrial activity and whole animal respiration in a common intertidal triplefin fish, *Forsterygion lapillum* (Family: Tripterygiidae). *J. Comp. Physiol. B Biochem. Syst. Environ. Physiol.* **184**, 991-1001. doi:10.1007/s00360-014-0861-9
Kleckner, N. W. and Sidell, B. D. (1985). Comparison of maximal activities of enzymes from tissues of thermally acclimated and naturally acclimatized chain pickerel (*Esox niger*). *Physiol. Zool.* **58**, 18-28. doi:10.1086/physzool.58.1.30161216
Little, A. G., Lau, G., Mathers, K. E., Leary, S. C. and Moyes, C. D. (2018). Comparative biochemistry of cytochrome c oxidase in animals. *Comp. Biochem. Physiol. Part B Biochem. Mol. Biol.* **224**, 170-184. doi:10.1016/j.cbpb.2017.11.005
Michaelsen, J., Fago, A. and Bundgaard, A. (2021). High temperature impairs mitochondrial function in rainbow trout cardiac mitochondria. *J. Exp. Biol.* **224**, jeb242382. doi:10.1242/jeb.242382
Morozov, S., Scott McCairns, R. J. and Merilä, J. (2019). FishResp: R package and GUI application for analysis of aquatic respirometry data. *Conserv. Physiol.* **7**, coz003. doi:10.1093/conphys/coz003
Nicholls, D. G. (2021). Mitochondrial proton leaks and uncoupling proteins. *Biochim. Biophys. Acta Bioenerg.* **1862**, 148428. doi:10.1016/j.bbabio.2021.148428
Norin, T. and Clark, T. D. (2016). Measurement and relevance of maximum metabolic rate in fishes. *J. Fish Biol.* **88**, 122-151. doi:10.1111/jfb.12796
Norin, T. and Malte, H. (2012). Intraspecific variation in aerobic metabolic rate of fish: Relations with organ size and enzyme activity in brown trout. *Physiol. Biochem. Zool.* **85**, 645-656. doi:10.1086/665982
O'Brien, K. M. (2011). Mitochondrial biogenesis in cold-bodied fishes. *J. Exp. Biol.* **214**, 275-285. doi:10.1242/jeb.046854
O'Brien, K. M., Rix, A. S., Egginton, S., Farrell, A. P., Crockett, E. L., Schlauch, K., Woolsey, R., Hoffman, M. and Merriman, S. (2018). Cardiac mitochondrial metabolism may contribute to differences in thermal tolerance of red- and white-blooded Antarctic notothenioid fishes. *J. Exp. Biol.* **221**, jeb177816. doi:10.1242/jeb.177816
Orczewska, J. I., Hartleben, G. and O'Brien, K. M. (2010). The molecular basis of aerobic metabolic remodeling differs between oxidative muscle and liver of threespine sticklebacks in response to cold acclimation. *Am. J. Physiol. Regul. Integr. Comp. Physiol.* **299**, R352-R364. doi:10.1152/ajpregu.00189.2010
Pamenter, M. E., Lau, G. Y. and Richards, J. G. (2018). Effects of cold on murine brain mitochondrial function. *PLoS One* **13**, 1-12. doi:10.1371/journal.pone.0208453
Pichaud, N., Ekström, A., Hellgren, K. and Sandblom, E. (2017). Dynamic changes in cardiac mitochondrial metabolism during warm acclimation in rainbow trout. *J. Exp. Biol.* **220**, 1674-1683. doi:10.1242/jeb.152421
Pichaud, N., Ekström, A., Breton, S., Sundström, F., Rowinski, P., Blier, P. U. and Sandblom, E. (2019). Cardiac mitochondrial plasticity and thermal sensitivity in a fish inhabiting an artificially heated ecosystem. *Sci. Rep.* **9**, 17832. doi:10.1038/s41598-019-54165-3
Porter, R. K., Hulbert, A. J. and Brand, M. D. (1996). Allometry of mitochondrial proton leak: influence of membrane surface area and fatty acid composition. *Am. J. Physiol. Regul. Integr. Comp. Physiol.* **271**, R1550-R1560. doi:10.1152/ajpregu.1996.271.6.R1550
Reemeyer, J. E. and Rees, B. B. (2019). Standardizing the determination and interpretation of P_{crit} in fishes. *J. Exp. Biol.* **222**, jeb210633. doi:10.1242/jeb.210633
Reeve, C., Rowsey, L. E. and Speers-Roesch, B. (2022). Inactivity and the passive slowing effect of cold on resting metabolism as the primary drivers of energy savings in overwintering fish. *J. Exp. Biol.* **225**, jeb243407. doi:10.1242/jeb.243407
Ressel, K. N., Cominassi, L., Sarrimanolis, J. and O'Brien, K. M. (2022). Aerobic scope is not maintained at low temperature and is associated with cardiac aerobic capacity in the three-spined stickleback *Gasterosteus aculeatus*. *J. Fish Biol.* **100**, 444-453. doi:10.1111/jfb.14955
Rolfe, D. F. S. and Brown, G. C. (1997). Cellular energy utilization and molecular origin of standard metabolic rate in mammals. *Physiol. Rev.* **77**, 731-758. doi:10.1152/physrev.1997.77.3.731
Rosewarne, P. J., Wilson, J. M. and Svendsen, J. C. (2016). Measuring maximum and standard metabolic rates using intermittent-flow respirometry: a student laboratory investigation of aerobic metabolic scope and environmental hypoxia in aquatic breathers. *J. Fish Biol.* **88**, 265-283. doi:10.1111/jfb.12795
Rummer, J. L., Binning, S. A., Roche, D. G. and Johansen, J. L. (2016). Methods matter: considering locomotory mode and respirometry technique when estimating metabolic rates of fishes. *Conserv. Physiol.* **4**, cow008. doi:10.1093/conphys/cow008

Salin, K., Auer, S. K., Rudolf, A. M., Anderson, G. J., Selman, C. and Metcalfe, N. B. (2016). Variation in metabolic rate among individuals is related to tissue-specific differences in mitochondrial leak respiration. *Physiol. Biochem. Zool.* **89**, 511-523. doi:10.1086/688769

Sandblom, E., Gräns, A., Axelsson, M. and Seth, H. (2014). Temperature acclimation rate of aerobic scope and feeding metabolism in fishes: implications in a thermally extreme future. *Proc. R. Soc. B Biol. Sci.* **281, 20141490**. doi:10.1098/rspb.2014.1490

Scheuffele, H., Rubio-Gracia, F. and Clark, T. D. (2021). Thermal performance curves for aerobic scope in a tropical fish (*Lates calcarifer*): flexible in amplitude but not breadth. *J. Exp. Biol.* **224**, jeb243504. doi:10.1242/jeb.243504

Song, J., Brill, R. W. and McDowell, J. R. (2019). Plasticity in standard and maximum aerobic metabolic rates in two populations of an estuarine dependent teleost, spotted seatrout (*Cynoscion nebulosus*). *Biology (Basel)* **8**, 46. doi:10.3390/biology8020046

Srere, P. A., Brazil, H., Gonen, L. and Takahashi, M. (1963). The citrate condensing enzyme of pigeon breast muscle and moth flight muscle. *Acta Chem. Scand.* **17** Supl., 129-134. doi:10.3891/acta.chem.scand.17s-0129

Steinhausen, M. F., Sandblom, E., Eliason, E. J., Verhille, C. and Farrell, A. P. (2008). The effect of acute temperature increases on the cardiorespiratory performance of resting and swimming sockeye salmon (*Oncorhynchus nerka*). *J. Exp. Biol.* **211**, 3915-3926. doi:10.1242/jeb.019281

Vézina, D. and Guderley, H. (1991). Anatomic and enzymatic responses of the three-spined stickleback, *Gasterosteus aculeatus*, to thermal acclimation and acclimatization. *J. Exp. Zool.* **258**, 277-287. doi:10.1002/jez.1402580302

Whoriskey, F. G. and Wootton, R. J. (1987). The swimming endurance of threespine sticklebacks, *Gasterosteus aculeatus* L., from the Afon Rheidol, Wales. *J. Fish Biol.* **30**, 335-339. doi:10.1111/j.1095-8649.1987.tb05757.x

Wootton, R. J. (1984). *A Functional Biology of Sticklebacks*. Springer US.

Wuitchik, S. J. S., Mogensen, S., Barry, T. N., Paccard, A., Jamniczky, H. A., Barrett, R. D. H. and Rogers, S. M. (2022). Evolution of thermal physiology alters the projected range of threespine stickleback under climate change. *Mol. Ecol.* **31**, 2312-2326. doi:10.1111/mec.16396

Yan, Y. and Xie, X. (2011). Liver mitochondrial and whole-animal level metabolic compensation in a catfish during seasonal acclimatization. *Curr. Zool.* **57**, 109-115. doi:10.1093/czoolo/57.1.109

Yan, Y. and Xie, X. (2015). Metabolic compensations in mitochondria isolated from the heart, liver, kidney, brain and white muscle in the southern catfish (*Silurus meridionalis*) by seasonal acclimation. *Comp. Biochem. Physiol. A Mol. Integr. Physiol.* **183**, 64-71. doi:10.1016/j.cbpa.2014.12.011

Zhang, Y., Gilbert, M. J. H. and Farrell, A. P. (2019). Finding the peak of dynamic oxygen uptake during fatiguing exercise in fish. *J. Exp. Biol.* **222**, jeb196568. doi:10.1242/jeb.196568